

2001

Laser Stabilization at 1536 nm Using Regenerative Spectral Hole Burning

P B. Sellin

N M. Strickland

Thomas Böttger

University of San Francisco, tbottger@usfca.edu

J L. Carlsten

R L. Cone

Follow this and additional works at: <http://repository.usfca.edu/phys>

 Part of the [Physics Commons](#)

Recommended Citation

Sellin, P.B., Strickland, N.M., Böttger, T., Carlsten, J.L., Cone, R.L. Laser stabilization at 1536 nm using regenerative spectral hole burning. (2001) *Physical Review B - Condensed Matter and Materials Physics*, 63 (15), art. no. 155111. <https://doi.org/10.1103/PhysRevB.63.155111>

This Article is brought to you for free and open access by the College of Arts and Sciences at USF Scholarship: a digital repository @ Gleeson Library | Geschke Center. It has been accepted for inclusion in Physics and Astronomy by an authorized administrator of USF Scholarship: a digital repository @ Gleeson Library | Geschke Center. For more information, please contact repository@usfca.edu.

Laser stabilization at 1536 nm using regenerative spectral hole burning

P. B. Sellin, N. M. Strickland,* T. Böttger, J. L. Carlsten, and R. L. Cone
Department of Physics, Montana State University, Bozeman, Montana 59717

(Received 31 August 2000; published 30 March 2001)

Laser frequency stabilization giving a 500-Hz Allan deviation for a 2-ms integration time with drift reduced to 7 kHz/min over several minutes was achieved at 1536 nm in the optical communication band. A continuously regenerated spectral hole in the inhomogeneously broadened ${}^4I_{15/2}(1) \rightarrow {}^4I_{13/2}(1)$ optical absorption of an $\text{Er}^{3+}:\text{Y}_2\text{SiO}_5$ crystal was used as the short-term frequency reference, while a variation on the locking technique allowed simultaneous use of the inhomogeneously broadened absorption line as a long-term reference. The reported frequency stability was achieved without vibration isolation. Spectral hole burning frequency stabilization provides ideal laser sources for high-resolution spectroscopy, real-time optical signal processing, and a range of applications requiring ultra-narrow-band light sources or coherent detection; the time scale for stability and the compatibility with spectral hole burning devices make this technique complementary to other frequency references for laser stabilization.

DOI: 10.1103/PhysRevB.63.155111

PACS number(s): 42.60.Lh, 42.62.Fi, 42.50.Md, 06.30.Ft

I. INTRODUCTION

Frequency-stable lasers are required for high-resolution spectroscopy¹ of solids, molecules, and atoms, for solid-state optoelectronic devices based on spectral hole burning² (SHB) such as GHz-scale time-domain optical signal processing³⁻⁶ and network packet switching,^{7,8} for precision laser ranging, long-baseline interferometry, and gravitational wave detection, for spatial coordination of satellite arrays, and for optical communication using coherent light detection. Such lasers are also suitable for sensitive vibration monitoring devices and a variety of other optical and fiber optical sensors.

We have demonstrated recently that persistent spectral holes⁹ and regenerative spectral holes¹⁰ burned in the absorption lines of Tm^{3+} -doped insulating crystals at 798 nm and 793 nm provide frequency references for laser stabilization with 500-Hz and 20-Hz Allan deviation for 10-ms integration times. Spectral holes provide alternatives that are complementary to precision atomic resonances¹¹ or reflection modes of Fabry-Perot optical cavities.^{12,13} Our demonstrations were carried out with crystals cooled to liquid-helium temperatures, but higher temperature operation at 15–20 K with 1-kHz frequency stability can be projected for the material of Ref. 9. Best performance with atomic resonances or Fabry-Perot cavities also typically requires liquid-helium temperatures.^{11,12}

The availability of ultranarrow SHB resonances down to 15 Hz in rare earth doped crystals, the relative immunity of spectral holes to environmental disturbances such as vibrations, and the portability and compactness of a stable laser system using SHB references with a closed-cycle cryocooler are important features that should enable application in a variety of fields beyond those normally associated with spectral hole burning. Stabilization of mode-locked lasers¹⁴ to spectral holes also should be practical and will have applications in the signal processing situations discussed above and in other contexts that require short pulses, frequency combs, or optical clocks. The SHB frequency references are well suited to applications where multiple frequencies are re-

quired and where the programmability of SHB materials allows programmable frequency differences up to the multi-GHz range or, if disordered solids are used, to the THz range. With the development of suitable photon-gated (or two-photon) SHB materials, the production of long-term secondary frequency standards based on SHB may become practical.

When stabilized laser sources are required for real-time optical signal processing in SHB materials, the use of a second piece of the same signal processing material as a SHB frequency reference provides automatic frequency compatibility between the signal processing material and the stabilized laser source.¹⁰ The relative vibrational immunity of the spectral holes provides an important simplification in system design and performance for either spectroscopy or SHB devices; this advantage is even greater when both the frequency reference and spectroscopic sample or SHB device are mounted on the same platform or sample holder. This has been demonstrated here for $\text{Er}^{3+}:\text{Y}_2\text{SiO}_5$. A stabilized laser of this type would be especially helpful, for example, in measurements of spectral diffusion¹⁵ using the stimulated photon echo technique.

The importance of stabilization in SHB signal processing is underscored by the observation that early moderate-speed demonstrations have been limited by laser frequency jitter that led to a loss in signal fidelity.³⁻⁸ These problems can occur at several levels: (a) uncontrolled phase variations between programming pulses when repeated pulse sequences are used for writing or refreshing spectral interference gratings, (b) the more extreme case where the jitter exceeds the Fourier width of the exciting pulses so that the processed pulses fail to overlap spectrally with the programming pulses, and similarly (c) the case where the jitter exceeds the Fourier width of the exciting pulses so that the excitation pulses fail to overlap spectrally with the probe pulse in measurements of spectral diffusion.¹⁵ Lasers stabilized to spectral holes are already playing an important role in proof-of-principle demonstrations of a variety of SHB devices.⁶

In this paper, an Er^{3+} -doped SHB crystal has been used to demonstrate laser stabilization in the important 1.5- μm tele-

communications band. Studies have shown^{15,16} that Er^{3+} -doped crystals have the frequency selectivity required for optical storage, real-time address header decoding for all-optical packet routing,^{7,8} and all-optical correlation.⁴⁻⁶ Since the laser in the present report is stabilized to the same transition used in those device demonstrations, the requirements of frequency overlap, frequency and phase stability, and time scale of stabilization are all automatically fulfilled, as mentioned earlier. The limits on device performance are set then by material parameters rather than by instability of the laser.^{10,15,16}

The stabilized-diode-laser- $\text{Er}^{3+}:\text{Y}_2\text{SiO}_5$ system described here exploits the regenerative SHB technique reported earlier.¹⁰ A transient spectral hole is continuously regenerated by the stabilized laser and provides a frequency reference at an arbitrarily chosen location in the inhomogeneous $\text{Er}^{3+}:\text{Y}_2\text{SiO}_5$ absorption profile. The stability of the laser will then be determined by the dynamical properties of the SHB material together with the design of the locking system.

To substantially improve the long-term frequency stability, we have extended the locking technique by using a combination of the error signal contributions from the spectral hole and the inhomogeneous line. The reduction of longer-term drift to 7 kHz/min over several minutes obtained with the extended technique represents a substantial improvement over the 600 kHz/min reported for $\text{Tm}:\text{YAG}$ (yttrium aluminum garnet).¹⁰ In the old and new cases, anticipated refinements to the feedback system and frequency modulators may be expected to provide further substantial improvement over both the long and the short term stability reported here, which is already 10^3 times better over important integration time scales than that for commercial lasers. As shown in Ref. 10, this provides new capabilities to probe dynamics in the neighborhood of the active rare-earth ions in SHB materials and to reveal small scale level structures and dynamics out to the tens of milliseconds scale or even longer.

II. $\text{Er}^{3+}:\text{Y}_2\text{SiO}_5$ MATERIAL PROPERTIES

The SHB crystal chosen as a frequency reference was $\text{Er}^{3+}:\text{Y}_2\text{SiO}_5$ with an Er^{3+} concentration of 0.005 at.%. This material exhibits transient spectral hole burning on the $^4I_{15/2}(1) \rightarrow ^4I_{13/2}(1)$ transitions at 1536.14 nm (site 1) and 1538.57 nm (site 2) by population storage in the excited state of the optically active ion.¹⁵ The inhomogeneous linewidth $\Gamma_{\text{inh}} = 500 \text{ MHz} = 0.017 \text{ cm}^{-1}$ is illustrated in Fig. 1, where a single spectral hole has also been burned into the line. The homogeneous linewidth Γ_h of this Er^{3+} transition decreases substantially in applied magnetic fields, leading to narrower spectral hole widths. The homogeneous linewidth for this crystal was determined from the optical dephasing time T_2 obtained from two-pulse photon echo decay experiments at 1.6 K, and the measured value $\Gamma_h \sim 5 \text{ kHz}$ is consistent with previously published results.¹⁵ Stronger magnetic fields have reduced the homogeneous linewidth to 78 Hz,¹⁶ and it is expected that further elucidation of the angular dependence of the Zeeman splittings will reveal a field direction that provides more rapid freezing out of electronic spin flips in-

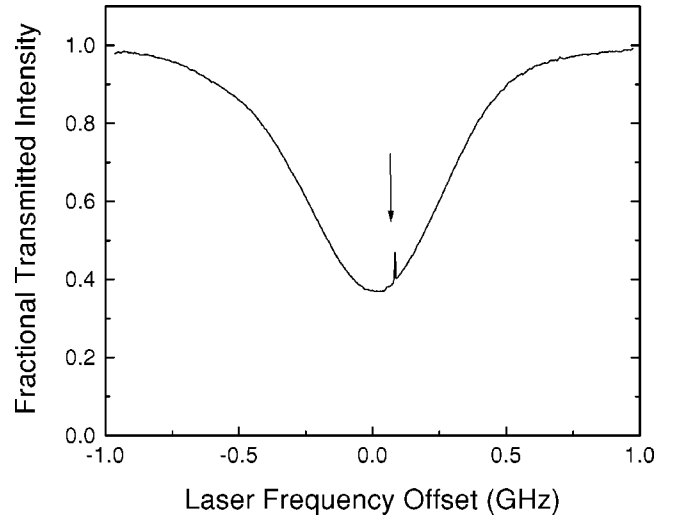


FIG. 1. Transmission spectrum of 0.005% $\text{Er}^{3+}:\text{Y}_2\text{SiO}_5$ scanned by a diode laser showing the entire inhomogeneously broadened absorption profile at zero applied field ($B=0 \text{ T}$). The arrow indicates a spectral hole burned by a second laser.

volving the excited component of the ground state and thus allow the linewidth to more closely approach the T_1 lifetime limited value of 15 Hz. In principle, the minimum linewidth of a shallow spectral hole burned by a narrow-band laser is $2\Gamma_h$ due to convolution of burning and reading cycles; deeper holes can be expected to become broader, since there is less saturation of material absorption in the wings of a hole than at the center.

The frequency-locking experiments reported here were performed using the strongest absorption transition from the lowest Zeeman-split level for site 1 in moderate magnetic fields of $B=0.2$ to 0.5 T ; the 0.2 T magnetic field value was chosen to simulate field strengths that have been obtained using compact 1-cm dia. Nd-Fe-B permanent magnets.^{5,8} The homogeneous linewidth at 0.5 T is about half that at 0.2 T .

Two frequency reference crystals were cut from the same crystal boule to give a linear inhomogeneously broadened absorption of $\sim 50\%$ at line center. Crystal dimensions were 5 mm (and 4 mm) along D_1 , 6 mm (and 5 mm) along D_2 , and 1 mm (and 1.2 mm) along b . Each crystal was oriented with its D_1 axis parallel to the magnetic field, the lasers' k -vectors parallel to the b axis, and the lasers polarized with E along D_2 . Both crystals were immersed in superfluid helium at 1.6 K in a single Dewar with a superconducting magnet that provided for adjustment of the magnetic field. The laser beams were spatially separated, and the crystals were masked so that each crystal was exposed to only one beam. The spectral holes were created with irradiances of $100 \mu\text{W}/\text{cm}^2$ using $\sim 3 \text{ mm}$ beam diameters. Beam irradiance was controlled using a $\lambda/2$ plate and a prism polarizer.

III. LOCKING TO A REGENERATIVE SPECTRAL HOLE

The experimental apparatus shown in Fig. 2 was similar to that described previously.^{9,10} Two external cavity diode lasers in the Littman-Metcalf configuration¹⁷ were equipped

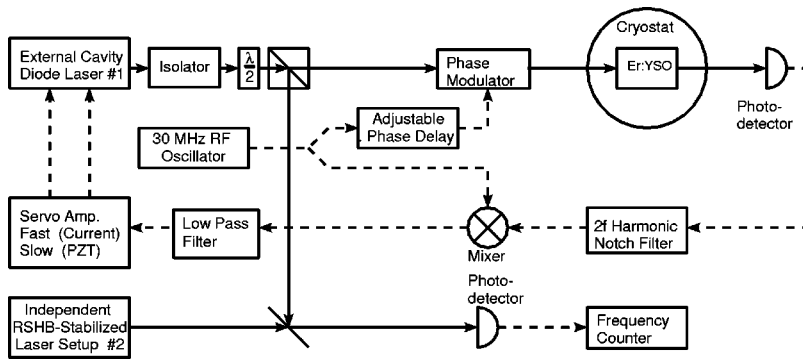


FIG. 2. Experimental apparatus for laser frequency locking to spectral holes and beat frequency measurement of laser stability (by combining the beam from the laser shown and that from an independent second laser system).

with $\text{In}_x\text{Ga}_{1-x}\text{As}_y\text{P}/\text{InP}$ quantum well diodes that had one facet angled to eliminate intracavity optical feedback.¹⁸ The Pound-Drever-Hall technique¹⁹ was used for locking the laser frequency to the spectral hole. The error signal was derived from the spectral hole transmission using frequency modulation (FM) spectroscopy,²⁰ with the two lasers modulated by external electro-optic modulators driven at 27 MHz and 30 MHz, respectively. These frequencies greatly exceeded the spectral hole widths but were far less than the inhomogeneous absorption linewidth $\Gamma_{\text{inh}}=500$ MHz. The primary laser side bands had a modulation index $M=0.4$, and secondary side bands were small but observable. The sharp resonance of the spectral hole in the inhomogeneous absorption line creates a corresponding dispersion in the refractive index. Figure 3(a) displays the transmission spectrum through a single spectral hole in the inhomogeneously broadened absorption profile for a phase-modulated laser (including side bands), and Fig. 3(b) plots the demodulated FM-spectroscopy error signals obtained simultaneously for three values of relative phase. In the stabilization system, each locking laser burns a hole in its reference crystal, primarily at

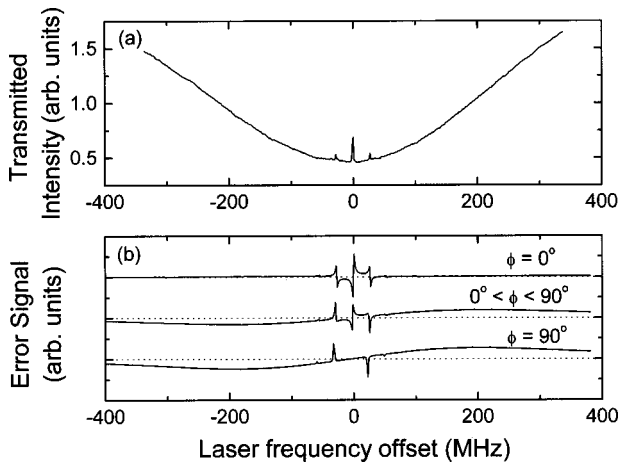


FIG. 3. (a) Transmission spectrum, as probed by a phase-modulated laser with sidebands, of a single spectral hole burned in the inhomogeneously broadened absorption profile by an unmodulated second laser, in an applied field of $B=0.2$ T. (b) Error signals derived from the spectral hole and the inhomogeneous line using different phase-delay settings. The spectral hole is not limited to line center as chosen for illustration in this particular figure but can also occupy other positions in the inhomogeneous line.

the carrier frequency but also at the frequencies of the FM side bands.

The FM error signal was processed by a servo loop that provided both fast corrections to the injection current of the laser diode and reduced bandwidth signals to the piezoelectric control of the laser's external diffraction grating. Control of the grating keeps the current servo within its operating limits. Due to laboratory constraints, the two lasers were on one table, and the reference crystals, magnet Dewar, and locking-beam detectors were on a separate table. Neither table was pneumatically floated, so the results reported here demonstrate the immunity of this locking technique to vibrations. By contrast, most other frequency references require extreme vibration isolation measures to reach this short-term stability.

Evaluation of the frequency stability of a single laser at sub-MHz resolution is difficult if one lacks a frequency standard at the appropriate wavelength for comparison. For that reason, two independent lasers were constructed and locked to two separate SHB crystal references. The frequency stability was determined by beating unmodulated portions of the two stabilized laser beams on a photodiode detector, recording the beat frequency measured by a commercial frequency counter, and carrying out subsequent statistical analysis of the time dependence of the beats using a computer.

The stability over broad time scales is characterized by the Allan deviation²¹ of the heterodyne beat frequency. Performance of the free-running lasers is shown in Fig. 4(a), while that of the lasers locked to regenerative spectral holes using the method of Ref. 10 is shown in Fig. 4(b). Short-term stabilization giving a 500-Hz Allan deviation for a 2-ms integration time was achieved with the conventional adjustment of the phase-sensitive error signal, that is, with the detector signal and local oscillator in phase at the mixer as illustrated by the $\phi=0^\circ$ signal of Fig. 3(b). Under these conditions, the dominant contribution to the error signal comes from the spectral hole. Comparison of the curves in Fig. 4(a) and Fig. 4(b) shows that slow frequency drift (integration times longer than 100 ms) of the stabilized lasers in these early experiments approached that of the unstabilized laser. Much of this drift is attributable to slowly varying dc voltage offsets in the feedback servo loop arising from residual amplitude modulation at the optical phase modulators and temperature drift in the feedback electronics¹⁰ and modulators. The servo offsets cause the laser to lock off-

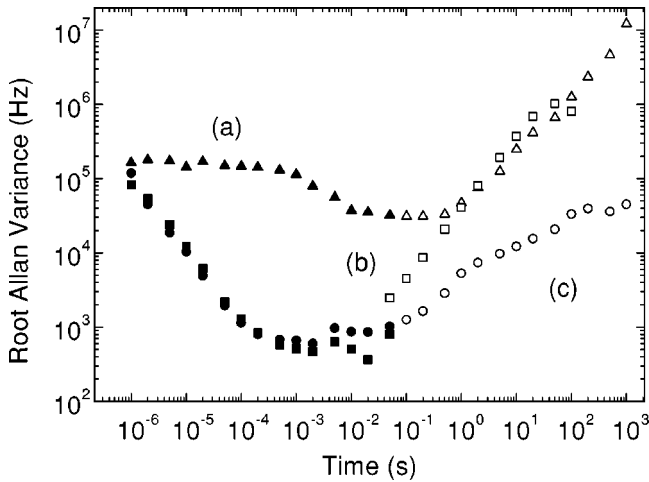


FIG. 4. Allan deviation values for the beat between two lasers: (a) lasers free running (triangles), (b) locked to spectral holes in different crystals using straight quadrature detection of the error signal at applied field $B=0.5$ T (squares), and (c) locked to spectral holes using the strategy of intermediate phase detection of the combined error signal from the spectral hole and inhomogeneous line at applied field $B=0.2$ T (circles). Filled symbols, 300 sample Allan deviations measured directly by a frequency counter; open symbols, values computed directly from beat-frequency data (cf. Fig. 5).

center to the spectral hole and consequently cause the regenerated spectral hole to drift continuously until the drift in the voltage offset undergoes a change of sign. Further development of the feedback servo system should substantially reduce these slowly varying offsets and thus reduce this long-term drift.

IV. INCORPORATING THE ABSORPTION LINE AS A FIXED REFERENCE

A locking strategy was devised, however, to reduce drift even with the existing servo system by simultaneously exploiting the high-resolution short-term frequency reference of the spectral hole and the long-term stability of the significantly broader inhomogeneous absorption line. Figure 3(b) illustrates the variation of the error signal as the relative phase between the detector signal and the local oscillator is varied through 90° at the mixer, with the multiple sharp features due to the narrow spectral hole superimposed on the broad background of the inhomogeneous line. The relative position of these two contributions on the frequency axis depends on the arbitrarily chosen position of the spectral hole. Crystal transmission is increased at the frequency of the spectral hole, so the transmission property of the hole and inhomogeneous absorption line have opposite signs. Their pure absorptive and dispersive FM contributions also have opposite signs in simple limiting cases. The shape of the FM signals, however, also depends on the relationship between the modulation frequency ν_m and the width of the relevant spectral feature. There is broad latitude for making this choice, since the hole width $\sim 2\Gamma_h$ can be from 10^5 to 10^8 times narrower than the inhomogeneous linewidth Γ_{inh} . In the present case, the linewidths of the hole contribution and

inhomogeneous line contribution lie at opposite extremes relative to the modulation frequency: $\Gamma_h \ll \nu_m \ll \Gamma_{inh}$. The two contributions to the error signal at line center are then strongly phase dependent and are maximized for different quadratures—the dispersive case for the spectral hole and absorptive case for the inhomogeneous profile. These phases are represented as 0° and 90° , respectively, in Fig. 3(b) and correspond to the $S2$ and $S1$ phases of Ref. 20. For a phase angle of $\phi=0^\circ$ the inhomogeneous line signal is negligible and the locking signal is derived primarily from the spectral hole and for a phase angle of $\phi=90^\circ$ the signal from the inhomogeneous line is maximized, but the contribution from the spectral hole has vanished at the line center of the hole. By choosing an intermediate phase $0^\circ < \phi < 90^\circ$, both contributions to the error signal contribute to locking stability; a steeply sloped signal from the spectral hole drives the short-term stability while at the same time a signal of lower slope from the inhomogeneous line opposes long-term drift.

With this procedure, the introduction of a static dc offset in the servo loop leads to an equilibrium lock point where a balance occurs between the sloping contribution from the inhomogeneous line and the dc offset. Though not a perfect solution, this is preferable to the original situation where a dc offset caused the locking to be displaced toward one side of the hole and consequently caused a steady drift in hole position and laser frequency as regenerative hole burning took place asymmetrically. Drift in hole position and hence in laser frequency can still occur with the present strategy if the dc offset is slowly varying, but the impacts on stability are reduced. This tendency to settle into an equilibrium position instead of continuing to drift not only improves the long-term frequency stability but also provides a means to choose an arbitrary frequency within the inhomogeneous absorption profile as the stabilization frequency. To adjust the locking frequency, either the dc offset level or the local oscillator phase (and hence the contribution of the inhomogeneous line to the error signal slope) may be adjusted. The system initially drifts towards and then settles at the equilibrium frequency, where the offset cancels the FM signal. This behavior was verified by computer simulation and by direct observation using a probe laser to monitor the position of the spectral hole and the locked laser within the inhomogeneous line.

The impact of this hybrid locking strategy on frequency stability is shown in the Allan deviation plot of Fig. 4(c). There is no degradation of the short-term stability, and the long-term stability is improved dramatically for integration times of 100 ms to greater than 1000 s, with the improvement exceeding two orders of magnitude at the longer times. Evolution of the heterodyne beat frequency over a period of 30 min (1800 s) is shown in Fig. 5(a) when both lasers were free running and in Fig. 5(b) when both lasers were locked using this strategy. For integration times of 1 s and longer, the drift has been reduced to about 7 kHz/min over several minutes. For small integration times (solid circles, triangles, and squares of Fig. 4), the Allan deviation values were directly measured by the frequency counter; for long integration times (open circles, triangles, and squares of Fig. 4), the Allan deviation was computed from the beat frequency data

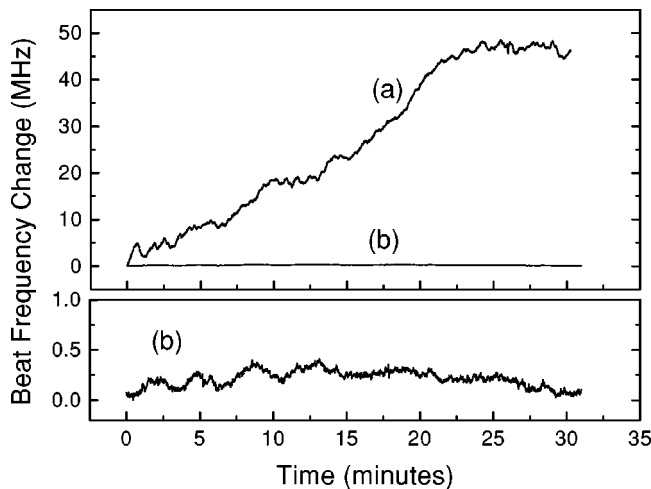


FIG. 5. Change in heterodyne beat signal between (a) free running and (b) independently locked lasers to separate spectral holes and inhomogeneous lines in different crystals at field $B=0.2$ T.

of Fig. 5, acquired at 50 ms intervals. The inherent sub-MHz free-running stability of the lasers is already sufficient for many spectroscopic applications, but an improvement over the free running case of about two orders of magnitude has been accomplished for time scales of 100 μ s–10 ms and for times longer than 1 min. Minimum Allan deviations of 200 Hz have been recorded, although the 500-Hz value in Fig. 4 is typical for performance at this stage of system development.

For somewhat stronger long-term resistance to drift, the modulation frequency could be increased to provide a larger inhomogeneous line contribution to the slope at the desired locking frequency; this increases the amplitude of the contribution from the inhomogeneous line with little effect on the contribution from the spectral hole.

The $\text{Er}^{3+}:\text{Y}_2\text{SiO}_5$ homogeneous resonance width in a magnetic field of 0.2 to 0.5 T is narrower^{15,16} than that from the preceding work¹⁰ on $\text{Tm}^{3+}:\text{YAG}$, so it might be expected to provide lower short-term Allan deviation values than $\text{Tm}^{3+}:\text{YAG}$ using the same technique and apparatus. In this case, however, the $4f^{11}$ electron configuration of the Er^{3+} ion leads to strong Er^{3+} magnetic moments, whereas the Tm^{3+} ion with configuration $4f^{10}$ has an electronic singlet ground state with “quenched” angular momentum and no first-order magnetic moment. Electron spin flips of nearby Er^{3+} ions in the ground state as well as nuclear spin flip-flops by Y^{3+} nuclei lead to fluctuations in the local fields and thus to measurable spectral diffusion^{15,16} of the Er^{3+} -ion population that make up the spectral hole frequency reference. The 0.2 to 0.5 T applied magnetic field reduces electron spin flips by reducing thermal population of the upper component of the Er^{3+} Kramers doublet ground state, but it does not eliminate them completely. It also suppresses the far weaker spectral diffusion due to Y^{3+} (or Er^{3+}) nuclear spin flip-flops. Evolution of the spectral hole width by spectral diffusion limits the currently achieved frequency stability of the hole on time scales longer than 2 ms and hence of the locked laser.

Further sources that limit stability are residual amplitude modulation²² produced by the electro-optic phase modulator and thermally induced drift in the locking circuitry and modulator, all of which introduce variable offsets to the error signal, causing the laser to lock slightly off the center of the spectral hole. In the previous implementation¹⁰ this produced unrestrained long-term frequency drift of the spectral hole. With the method reported here, it results instead in smaller changes to the equilibrium lock point in the inhomogeneous line profile. As noted above, further improvements from passively and actively stabilizing the temperature of the feedback electronics are expected to improve system performance.

V. IMPROVED PHOTON ECHO STABILITY FOR APPLICATIONS

Time-domain spectroscopy and a wide range of proposed SHB optical devices^{2–8} are based on the photon echo and stimulated photon echo, the capabilities of these techniques can be improved with the level of frequency stabilization reported here. For optimal exploitation of the stimulated photon echo, laser frequency stability to better than the spectral width of the broadest excitation pulse (or in the limiting case to better than a homogeneous linewidth) is required for the storage time of the material, which is defined by the decay time of a transient spectral hole for the transition being probed. With lasers stabilized to spectral holes, this requirement is naturally and automatically met.

Here we demonstrate this improvement by measuring stimulated photon echoes on the $^4I_{15/2}(1) \rightarrow ^4I_{13/2}(1)$ site (1) transition of $\text{Er}^{3+}:\text{Y}_2\text{SiO}_5$ using a stabilized 1536-nm laser, an Er-doped fiber amplifier, and the echo apparatus described previously.¹⁰ Approximately 5 mW of unmodulated continuous-wave laser power was available for producing echo excitation pulses after continuous-wave amplification of the laser by the Er-doped fiber amplifier, which was located outside the servo loop for laser stabilization. A portion of the unamplified laser output was used to frequency-lock the laser to a regenerative transient spectral hole in the same transition as described above. Echo excitation pulses were produced using two acousto-optic modulators in series to improve the on/off contrast ratio and to cancel any net shift in the laser frequency, since the $\text{Er}^{3+}:\text{Y}_2\text{SiO}_5$ spectral lines are narrow. The resulting photon echo signal was gated from the transmitted beam by a third acousto-optic modulator to discriminate against the exciting pulses. The echo was detected with a fast $\text{In}_x\text{Ga}_{1-x}\text{As}$ -photodiode. To generate stimulated photon echoes, three 2- μ s excitation pulses were incident on the crystal, with the delay t_{12} between the first and second pulses fixed at 19 μ s. The strength of the stimulated echo was measured as a function of the delay t_{23} between the second and third pulses.

With the laser frequency locked to a transient spectral hole, photon echoes could be measured consistently for t_{23} delay times of several hundreds of microseconds, giving the data in Fig. 6(b). The limiting factor for measuring echoes with longer t_{23} delay times was the detector signal-to-noise ratio rather than laser frequency jitter even though

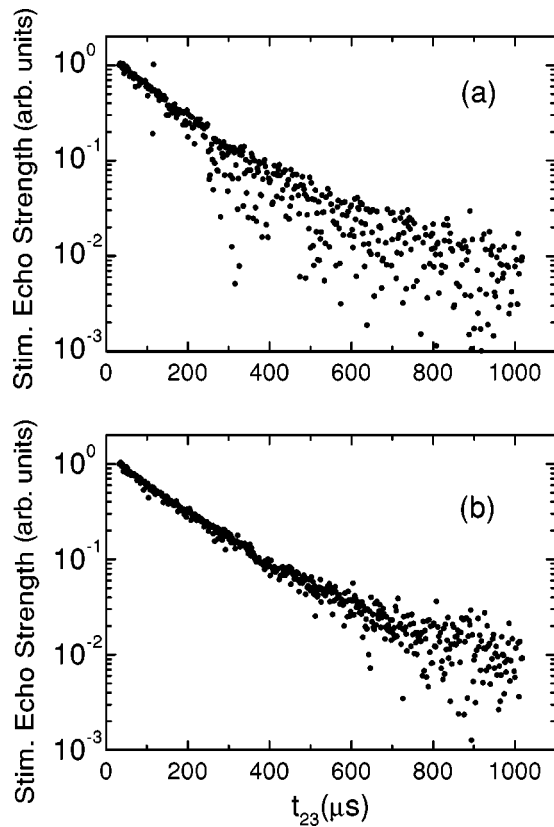


FIG. 6. Stimulated-photon-echo decay on the ${}^4I_{15/2}(1) \rightarrow {}^4I_{13/2}(1)$ transition in $\text{Er}^{3+}:\text{Y}_2\text{SiO}_5$. Each point represents a single shot. (a) Measured with a free-running laser. (b) Measured with a laser stabilized to a spectral hole and inhomogeneous line at field $B = 0.2$ T.

additional jitter may have been introduced by the Er-doped fiber amplifier. After 800- μs total delay time the stimulated echo signal was buried in the noise. In contrast, when the stimulated echo decay was measured with the laser free running, the reproducibility of the stimulated echo became unreliable after only 200 μs , as shown in Fig. 6(a). All the data points of Fig. 6 were single-shot acquisitions of the stimulated photon echo without thresholding to reject low-intensity echoes. Figure 6(a) demonstrates that frequency jit-

ter was the cause of the echo signal amplitude fluctuations when a free-running laser was used, since occasionally an optimum echo was produced when the laser frequency of the third pulse happened to match that of the first two. An envelope of “good” echoes can be seen, but most points fall well below this. Clearly, averaging the data in Fig. 6(a) over multiple shots would lead to a much different and erroneous echo decay rate.

VI. CONCLUSIONS

The concept of laser frequency stabilization using regenerative transient spectral hole burning has been extended to the technologically important 1.5- μm wavelength region. Stable laser sources based on this method improve both spectroscopic capability and the performance of SHB devices such as all-optical network routers and address header decoders. Moreover, by stabilizing the laser source to the same SHB material already employed in the SHB device, system complexity is significantly reduced. A hybrid method to control long-term frequency drift has been demonstrated, using an intermediate phase delay in the phase sensitive detection of the frequency locking error signal that exploits contributions from the narrow spectral hole and from the inhomogeneous absorption profile. This stabilization method is particularly well suited for spectroscopy and for optical data processing devices based on time-domain spectral hole burning. Substantial improvement in stimulated photon-echo reproducibility was demonstrated, showing the impact of this technique on spectroscopy of rare-earth materials.

As materials having gated persistent spectral holes with very long lifetimes are developed,²³ the locking techniques reported here for regenerative SHB can be applied to produce sources with long-term stability and perhaps provide highly portable secondary frequency standards.

ACKNOWLEDGMENTS

This research was supported by U.S. Air Force Office of Scientific Research Grant Nos. F49620-96-1-0466, F49620-98-1-0171, and F49620-99-1-0202. The $\text{Er}^{3+}:\text{Y}_2\text{SiO}_5$ crystals were provided by Scientific Materials Corporation of Bozeman, MT.

*Present address: Industrial Research Ltd., P.O. Box 31-310, Lower Hutt, New Zealand.

¹R. G. DeVoe and R. G. Brewer, *Phys. Rev. Lett.* **50**, 1269 (1983); R. M. Macfarlane and R. M. Shelby, in *Spectroscopy of Crystals Containing Rare-Earth Ions*, edited by A. A. Kaplyanskii and R. M. Macfarlane (North-Holland, Amsterdam, 1987); M. J. Sellars, R. S. Meltzer, P. T. H. Fisk, and N. B. Manson, *J. Opt. Soc. Am. B* **11**, 1468 (1994).

²T. W. Mossberg, *Opt. Lett.* **7**, 77 (1982); A. Rebane, R. Kaarli, P. Saari, A. Anijalg, and K. Timpmann, *Opt. Commun.* **47**, 173 (1983); M. Mitsunaga, R. Yano, and N. Uesugi, *Opt. Lett.* **16**, 1890 (1991); M. Mitsunaga, N. Uesugi, H. Sasaki, and K. Karaki, *ibid.* **19**, 752 (1994); H. Lin, T. Wang, and T. W. Mossberg, *ibid.* **20**, 1658 (1995).

³N. W. Carlson, L. J. Rothberg, A. G. Yodh, W. R. Babbitt, and

T. W. Mossberg, *Opt. Lett.* **8**, 483 (1983); M. Zhu, W. R. Babbitt, and C. M. Jefferson, *ibid.* **20**, 2514 (1995); K. D. Merkel and W. R. Babbitt, *ibid.* **24**, 172 (1999).

⁴T. R. Dyke, M. J. Sellars, G. J. Pryde, N. B. Manson, U. Elman, and S. Kröll, *J. Opt. Soc. Am. B* **16**, 805 (1999); G. J. Pryde, M. J. Sellars, and N. B. Manson, *Phys. Rev. Lett.* **84**, 1152 (2000); M. J. Sellars, G. J. Pryde, N. B. Manson, and E. R. Krausz, *J. Lumin.* **87**, 833 (2000).

⁵T. L. Harris, Y. Sun, W. R. Babbitt, R. L. Cone, J. A. Ritcey, and R. W. Equall, *Opt. Lett.* **25**, 85 (2000).

⁶K. D. Merkel, R. W. Peters, P. B. Sellin, K. S. Repasky, and W. R. Babbitt, *Opt. Lett.* **25**, 1627 (2000).

⁷X. A. Shen and R. Kachru, *Opt. Lett.* **20**, 2508 (1995); T. Wang, H. Lin, and T. W. Mossberg, *ibid.* **20**, 2541 (1995).

- ⁸T. L. Harris, Y. Sun, R. L. Cone, R. M. Macfarlane, and R. W. Equall, *Opt. Lett.* **23**, 636 (1998).
- ⁹P. B. Sellin, N. M. Strickland, J. L. Carlsten, and R. L. Cone, *Opt. Lett.* **24**, 1038 (1999).
- ¹⁰N. M. Strickland, P. B. Sellin, Y. Sun, J. L. Carlsten, and R. L. Cone, *Phys. Rev. B* **62**, 1473 (2000).
- ¹¹R. J. Rafac, B. C. Young, J. A. Beall, W. M. Itano, D. J. Wineland, and J. C. Bergquist, *Phys. Rev. Lett.* **85**, 2462 (2000).
- ¹²S. Seel, R. Storz, G. Ruoso, J. Mlynek, and S. Schiller, *Phys. Rev. Lett.* **78**, 4741 (1997).
- ¹³B. C. Young, F. C. Cruz, W. M. Itano, and J. C. Bergquist, *Phys. Rev. Lett.* **82**, 3799 (1999).
- ¹⁴R. J. Jones, J.-C. Diehls, J. Jasapara, and W. Rudolf, *Opt. Commun.* **175**, 409 (2000); S. A. Diddams, D. J. Jones, J. Ye, S. T. Cundiff, J. L. Hall, J. K. Ranka, R. S. Windeler, R. Holzwarth, T. Udem, and T. W. Hänsch, *Phys. Rev. Lett.* **84**, 5102 (2000).
- ¹⁵R. M. Macfarlane, T. L. Harris, Y. Sun, R. L. Cone, and R. W. Equall, *Opt. Lett.* **22**, 871 (1997).
- ¹⁶Y. Sun, R. L. Cone, T. L. Harris, R. M. Macfarlane, and R. W. Equall, *Bull. Am. Phys. Soc.* **43**, 526 (1998).
- ¹⁷K. Liu and M. G. Littman, *Opt. Lett.* **6**, 117 (1981); P. McNichol and H. J. Metcalf, *Appl. Opt.* **24**, 2757 (1985); K. C. Harvey and C. J. Myatt, *Opt. Lett.* **16**, 910 (1991).
- ¹⁸P. J. S. Heim, Z. F. Fan, S. H. Cho, K. Nam, M. Dagenais, F. G. Johnson, and R. Leavitt, *Electron. Lett.* **33**, 1387 (1997).
- ¹⁹R. W. P. Drever, J. L. Hall, F. V. Kowalski, J. Hough, G. M. Ford, A. J. Munley, and H. Ward, *Appl. Phys. B: Photophys. Laser Chem.* **31**, 97 (1983); M. Zhu and J. L. Hall, *J. Opt. Sci. Am. B* **10**, 802 (1993).
- ²⁰G. C. Bjorklund, M. D. Levenson, W. Lenth, and C. Ortiz, *Appl. Phys. B: Photophys. Laser Chem.* **32**, 145 (1983); J. M. Supplee, E. A. Whittaker, and W. Lenth, *Appl. Opt.* **33**, 6294 (1994).
- ²¹D. W. Allan, *IEEE Trans. Ultrason. Ferroelectr. Freq. Control* **34**, 647 (1987).
- ²²N. C. Wong and J. L. Hall, *J. Opt. Soc. Am. B* **2**, 1527 (1985); F. L. Walls, *IEEE Trans. Ultrason. Ferroelectr. Freq. Control* **34**, 592 (1987); R. W. Fox, L. D'Evelyn, H. G. Robinson, C. S. Weimer, and L. Hollberg, *Proc. SPIE* **2378**, 58 (1995).
- ²³C. W. Thiel, H. Cruguel, H. Wu, Y. Sun, G. J. Lapeyre, R. L. Cone, R. W. Equall, and R. M. Macfarlane (unpublished).